Physics Letters B 723 (2013) 172–176

Contents lists available at SciVerse ScienceDirect

Physics Letters B

www.elsevier.com/locate/physletb

β-decay half-lives of neutron-rich nuclei and matter flow in the r-process

Z.M. Niu [a,b], Y.F. Niu [b,c], H.Z. Liang [b,d], W.H. Long [e], T. Nikšić [f], D. Vretenar [f], J. Meng [b,g,h,*]

[a] School of Physics and Material Science, Anhui University, Hefei 230039, China
[b] State Key Laboratory of Nuclear Physics and Technology, School of Physics, Peking University, Beijing 100871, China
[c] Institute of Fluid Physics, China Academy of Engineering Physics, Mianyang 621900, China
[d] RIKEN Nishina Center, Wako 351-0198, Japan
[e] School of Nuclear Science and Technology, Lanzhou University, Lanzhou 730000, China
[f] Physics Department, Faculty of Science, University of Zagreb, Croatia
[g] School of Physics and Nuclear Energy Engineering, Beihang University, Beijing 100191, China
[h] Department of Physics, University of Stellenbosch, Stellenbosch 7602, South Africa

ARTICLE INFO

Article history:
Received 15 February 2013
Received in revised form 20 April 2013
Accepted 24 April 2013
Available online 27 April 2013
Editor: W. Haxton

ABSTRACT

The β-decay half-lives of neutron-rich nuclei with $20 \leqslant Z \leqslant 50$ are systematically investigated using the newly developed fully self-consistent proton–neutron quasiparticle random phase approximation (QRPA), based on the spherical relativistic Hartree–Fock–Bogoliubov (RHFB) framework. Available data are reproduced by including an isospin-dependent proton–neutron pairing interaction in the isoscalar channel of the RHFB + QRPA model. With the calculated β-decay half-lives of neutron-rich nuclei a remarkable speeding up of r-matter flow is predicted. This leads to enhanced r-process abundances of elements with $A \gtrsim 140$, an important result for the understanding of the origin of heavy elements in the universe.

Nuclear β-decay plays an important role not only in nuclear physics but also in other branches of science, notably astrophysics and particle physics. In nuclei the investigation of β-decay provides information on the spin and isospin dependence of the effective nuclear interaction, as well as on nuclear properties such as masses [1], shapes [2], and energy levels [3]. In nuclear astrophysics β-decay half-lives set the time scale of the rapid neutron-capture process (r-process), and hence determine the production of heavy elements in the universe [4–6]. In particle physics β-decay was used to obtain the first experimental evidence of parity violation [7], and can be utilized to verify the unitarity of the Cabibbo–Kobayashi–Maskawa (CKM) matrix [8,9].

Important advances in the measurement of nuclear β-decay half-lives have been achieved in recent years with the development of radioactive ion-beam facilities, especially for nuclei near the neutron shell closures of 50 and 82 [10–12]. Quite recently β-decay half-lives of very neutron-rich Kr to Tc isotopes with neutron number between $N = 50$ and 82 have been measured [13]. The new experimental results indicate a systematic deviation from half-lives predicted by standard calculations based on the finite-range droplet model (FRDM) plus quasiparticle random phase approximation (QRPA) [14]. The impact of newly measured β-decay half-lives on the r-process nucleosynthesis has been investigated in Ref. [15], and it has been shown that the main effect is an enhancement in the abundances of isotopes with mass number $A = 110$–120, relative to abundances calculated using β-decay half-lives estimated with the FRDM + QRPA.

Most neutron-rich nuclei relevant for the r-process are still out of experimental reach and, therefore, r-process calculations are based on theoretical predictions for β-decay half-lives. Theoretical investigations of the nuclear β-decay started in the 1930's with the famous Fermi theory [16]. Two types of microscopic approaches are nowadays mainly used in large-scale calculations of nuclear β-decay half-lives: the shell model and the proton–neutron QRPA. Specifically, the shell model has been applied to studies of β-decay half-lives for nuclei at neutron number $N = 50, 82, 126$, and the experimental half-lives are reproduced by calculations [6,17,18]. However, shell-model calculations for heavy nuclei away from the magic numbers are not feasible yet because of extremely large configuration spaces. Compared to this approach, the proton–neutron QRPA can be applied to arbitrary heavy systems. Nuclear β-decay calculations have been carried out using the QRPA based on the FRDM [14], the extended Thomas–Fermi plus Strutinsky integral (ETFSI) model [19], the Skyrme Hartree–Fock–Bogoliubov (SHFB) model [20], and the density functional of Fayans (DF) [21].

* Corresponding author at: State Key Laboratory of Nuclear Physics and Technology, School of Physics, Peking University, Beijing 100871, China.
E-mail address: mengj@pku.edu.cn (J. Meng).

0370-2693/$ – see front matter
http://dx.doi.org/10.1016/j.physletb.2013.04.048

Covariant density functional theory (CDFT) has been applied very successfully to the description of a variety of nuclear structure phenomena [22–24]. The CDFT framework naturally includes the nucleon spin degree of freedom, and the resulting nuclear spin–orbit potential automatically emerges with the empirical strength, thus producing a good agreement with the experimental single-nucleon spectrum [25]. Based on the relativistic Hartree–Bogoliubov (RHB) model in the CDFT framework, the QRPA has been formulated [26] and employed in the calculations of β-decay half-lives of neutron-rich nuclei in the regions of $N \approx 50$ and $N \approx 82$ [27,28].

To reliably predict properties of thousands of unknown nuclei relevant to the r-process, the self-consistency of the QRPA approach is essential. Only recently the fully self-consistent relativistic RPA has been formulated based on the relativistic Hartree–Fock (RHF) theory [29]. The RHF + RPA model produces results in excellent agreement with data on the Gamow–Teller (GTR) and spin-dipole resonances in doubly magic nuclei, without any readjustment of the parameters of the covariant energy density functional [29,30]. Recently also the relativistic Hartree–Fock–Bogoliubov (RHFB) theory has been developed, thus providing a unified description of both mean field and pairing correlations [31,32].

In this Letter we report the implementation of a fully self-consistent proton–neutron QRPA for spherical nuclei, based on the RHFB theory [31,32], and its first systematic application in calculations of β-decay half-lives of neutron-rich nuclei with $20 \leqslant Z \leqslant 50$, extending over the whole r-process path from $N = 50$ to $N = 82$. The effect on r-process nucleosynthesis simulations is also investigated using the classical r-process model.

The details of the QRPA formalism in the canonical basis can be found in Refs. [20,26]. In the RHFB + QRPA model both the direct and exchange terms are taken into account, so the matrix elements of the particle–hole (p–h) V^{ph} and particle–particle (p–p) V^{pp} residual interactions read, respectively,

$$V^{ph}_{pnp'n'} = \iint d\boldsymbol{r}_1\, d\boldsymbol{r}_2 f^+_p(\boldsymbol{r}_1) f^+_{n'}(\boldsymbol{r}_2) \sum_{\phi_i} V_{\phi_i}(1,2) \times \big[f_{p'}(\boldsymbol{r}_2) f_n(\boldsymbol{r}_1) - f_n(\boldsymbol{r}_2) f_{p'}(\boldsymbol{r}_1)\big], \quad (1)$$

$$V^{pp}_{pnp'n'} = \iint d\boldsymbol{r}_1\, d\boldsymbol{r}_2 f^+_p(\boldsymbol{r}_1) f^+_n(\boldsymbol{r}_2) \sum_{T=1,0} V_T(1,2) \times \big[f_{n'}(\boldsymbol{r}_2) f_{p'}(\boldsymbol{r}_1) - f_{p'}(\boldsymbol{r}_2) f_{n'}(\boldsymbol{r}_1)\big]. \quad (2)$$

p, p', and n, n' denote proton and neutron quasiparticle canonical states, respectively, and ϕ_i and T denote corresponding coupling channels. $f_{p(n)}$ are canonical wave functions extracted from the RHFB calculations.

Because of the presence of exchange terms, the proton–neutron QRPA interaction contains terms generated not only by the isovector meson exchange (ρ and π), but also by the exchange of isoscalar mesons (σ and ω). As in Ref. [29], the pionic zero-range counter term introduced to remove the contact part of the pseudovector π-N coupling, reads

$$V_{\pi\delta}(1,2) = g' \left[\frac{f_\pi}{m_\pi}\vec{\tau}\gamma_0\gamma_5\boldsymbol{\gamma}\right]_1 \cdot \left[\frac{f_\pi}{m_\pi}\vec{\tau}\gamma_0\gamma_5\boldsymbol{\gamma}\right]_2 \delta(\boldsymbol{r}_1 - \boldsymbol{r}_2), \quad (3)$$

where the self-consistency of the model requires $g' = 1/3$. For the isovector ($T = 1$) p–p channel the pairing part of the Gogny force D1S [33] is consistently used both in the RHFB and QRPA calculations. For the isoscalar ($T = 0$) proton–neutron pairing in the QRPA we employ a similar interaction that was previously used in Refs. [20,27,28]:

$$V_{T=0}(1,2) = -V_0 \sum_{j=1}^{2} g_j e^{-[(\boldsymbol{r}_1 - \boldsymbol{r}_2)/\mu_j]^2} \hat{\prod}_{S=1,T=0}, \quad (4)$$

with $\mu_1 = 1.2$ fm, $\mu_2 = 0.7$ fm, $g_1 = 1$, $g_2 = -2$. The operator $\hat{\prod}_{S=1,T=0}$ projects onto states with $S = 1$ and $T = 0$. V_0 is the overall strength of the $T = 0$ proton–neutron pairing. Experimental evidence for $T = 0$ proton–neutron pairing is supported by recent studies of the level structure of ^{92}Pd [34], and the high-spin isomer in ^{96}Cd [35].

With the individual transition strengths B_m obtained from QRPA calculations, the β-decay half-life of an even–even nucleus is calculated in the allowed Gamow–Teller approximation using the expression:

$$T_{1/2} = \frac{D}{g_A^2 \sum_m B_m f(Z, E_m)}, \quad (5)$$

where $D = 6163.4 \pm 3.8$ s and $g_A = 1$. The sum runs over all final states with an excitation energy smaller than the Q_β value. The integrated phase volume $f(Z, E_m)$ can be written as

$$f(Z, E_m) = \int_{m_e}^{E_m} p_e E_e (E_m - E_e)^2 F_0(Z, E_e)\, dE_e, \quad (6)$$

where p_e, E_e, and $F_0(Z, E_e)$ denote the momentum, energy, and Fermi function of the emitted electron, respectively [6]. The β-decay transition energy E_m, that is, the energy difference between the initial and final state, is calculated using the QRPA:

$$E_m = \Delta_{np} - E_{\mathrm{QRPA}}, \quad (7)$$

where E_{QRPA} is the QRPA energy with respect to the ground-state of the parent nucleus and corrected by the difference of the neutron and proton Fermi energies in the parent nucleus [20], and Δ_{np} is the neutron–proton mass difference.

Nuclear β-decay half-lives are very sensitive to the $T = 0$ proton–neutron pairing interaction, and its strength V_0 is determined by adjusting QRPA results to empirical half-lives [20,27,28]. Taking ^{70}Fe and ^{130}Cd as reference nuclei for the two mass regions, the value of V_0 is determined as 155 MeV and 255 MeV, respectively. Using these two values, the calculated half-lives of Fe and Cd isotopes are shown in Fig. 1. For comparison, the experimental values and the results of a calculation without the $T = 0$ pairing are also displayed. One notices that the β-decay half-lives calculated without the inclusion of $T = 0$ pairing are systematically much longer than the experimental half-lives, both for Fe and Cd isotopes. In previous studies a constant value of V_0 was taken for one isotopic chain or one mass region, determined by adjusting to the known half-lives of selected nuclei in the isotopic chain [27], or several nuclei in the same mass region [20]. This procedure, of course, limits the predictive power of the model. Moreover, as shown in Fig. 1, when V_0 is determined by the β-decay half-life of ^{130}Cd the calculated results underestimate the half-lives of ^{118,120,122}Cd. This indicates that the half-lives of an isotopic chain cannot always be reproduced using a constant value V_0, and points out to a possible isospin-dependence of V_0. In the present work, therefore, we employ the following ansatz for an isospin-dependent pairing strength:

$$V_0 = V_L + \frac{V_D}{1 + e^{a+b(N-Z)}}, \quad (8)$$

and adjust the parameters to reproduce the known half-lives of even–even nuclei with $20 \leqslant Z \leqslant 50$, and $N - Z$ in the range $8 \leqslant N - Z \leqslant 36$. The resulting values: $V_L = 134.0$ MeV, $V_D =$

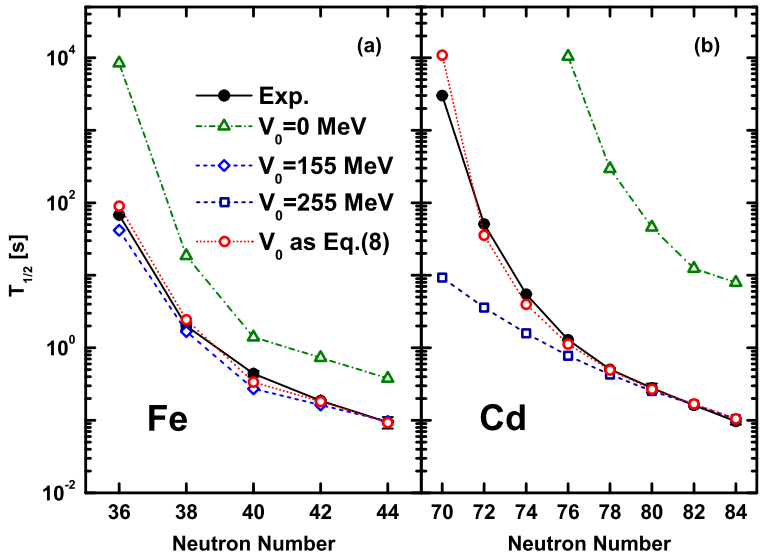

Fig. 1. (Color online.) Nuclear β-decay half-lives of Fe (left) and Cd (right) isotopes, calculated with the PKO1 effective interaction [36], compared to the experimental values [10]. Open triangles, diamonds, and squares denote values obtained using the RHFB + QRPA with the strength parameter of the $T = 0$ pairing: $V_0 = 0, 155,$ and 255 MeV, respectively. The RHFB + QRPA values obtained with the V_0 of Eq. (8) are denoted by open circles.

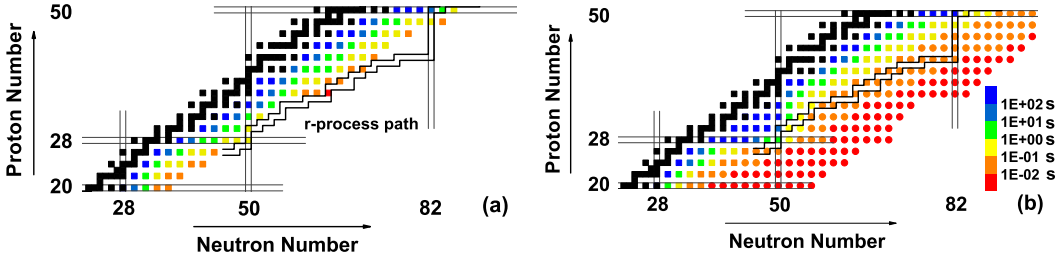

Fig. 2. (Color online.) Contour maps of β-decay half-lives for the $Z = 20$–50 even–even nuclei. The experimental half-lives [10,13] and the RHFB + QRPA results obtained with the effective interaction PKO1 are shown in the right (a) and left (b) panels, respectively. For reference, the r-process path calculated with the relativistic mean-field (RMF) mass model [38] is also included in the maps.

121.1 MeV, $a = 8.5$, and $b = -0.4$ are used in the calculation of β-decay half-lives for nuclei in the interval $8 \leqslant N - Z \leqslant 50$.

With the isospin-dependent strength Eq. (8) of the proton–neutron pairing interaction, the calculated β-decay half-lives of both the Fe and Cd isotopic chains are in excellent agreement with data. In the next step we proceed to calculate the half-lives of even–even nuclei with $20 \leqslant Z \leqslant 50$ using the RHFB + QRPA model, and compare the theoretical values to data in Fig. 2. Even though a wealth of new data on nuclear β-decay half-lives have been obtained in recent years, only few measurements can reach the r-process path, especially for r-process nuclei around $N = 82$. The present RHFB + QRPA calculation yields results in good agreement with the data, in particular for nuclei with half-lives $T_{1/2} < 1$ s. Only an overestimation of half-lives for Ni, Zn, and Ge isotopes near the stability line is noticed. The longer half-lives predicted for Ni isotopes is a common problem in self-consistent relativistic QRPA calculations [27,28]. For Zn and Ge isotopes, the differences between present results and the experimental values are remarkably reduced as the neutron number increases. Taking ^{84}Ge for example, the theoretical result is 1.3 s, rather close to the experimental value: 0.954 ± 0.014 s.

In Fig. 3, the calculated β-decay half-lives of a sequence of Cd isotopes using the RHFB + QRPA approach are displayed in comparison with measured values and previous theoretical results. One notices that the RHFB + QRPA model reproduces in detail the empirical β-decay half-lives, whereas the RHB + QRPA [27] and SHFB + QRPA [20] calculations that used a constant proton–neutron pairing strength cannot yield the appropriate isospin dependence of β-decay half-lives. The global FRDM + QRPA calculation [14] systematically overestimates the measured half-lives of Cd isotopes.

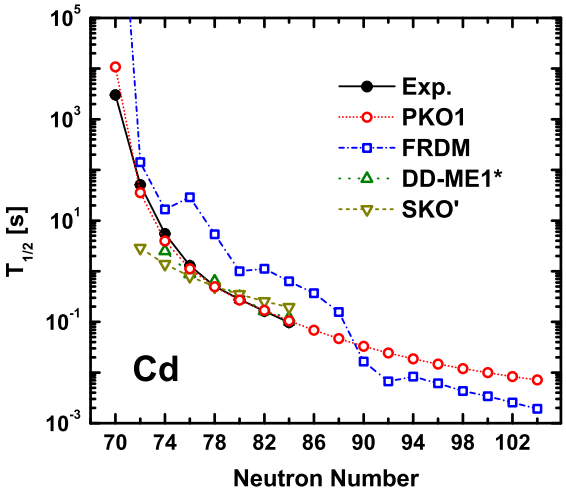

Fig. 3. (Color online.) Nuclear β-decay half-lives of Cd isotopes calculated in the RHFB + QRPA framework using the isospin-dependent proton–neutron pairing interaction, and the effective interaction PKO1. For comparison, the experimental values [10], as well as the theoretical results obtained in the RHB + QRPA model with the effective interaction DD-ME1* [27], the SHFB + QRPA calculation with the effective interaction SkO′ [20], and the FRDM + QRPA calculation [14], are also shown.

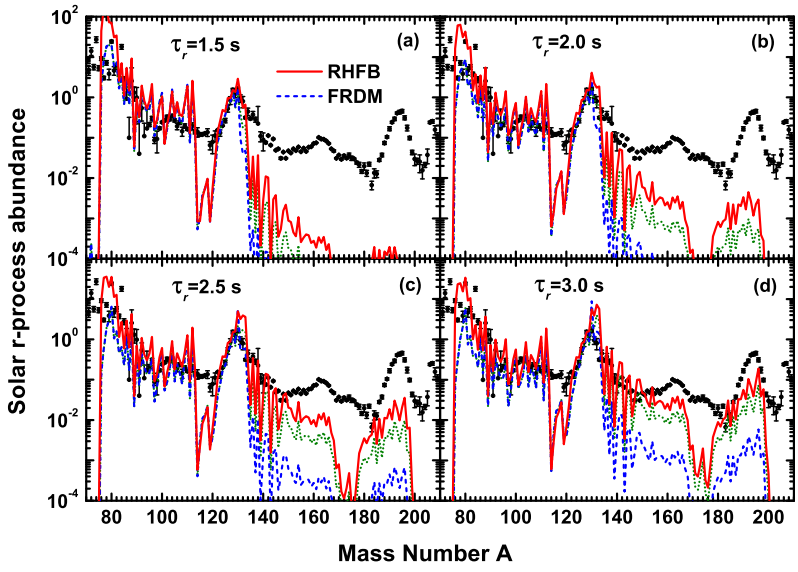

Fig. 4. (Color online.) The impact of nuclear β-decay half-lives on the r-matter flow. The solid (dashed) curves correspond to r-process abundances calculated with the RHFB + QRPA (FRDM + QRPA) β-decay half-lives in comparison to the data denoted by the points. The dotted curves are the same as the dashed curves but with half-lives of ^{130}Cd and ^{134}Sn replaced by the corresponding RHFB + QRPA results. In all calculations, nuclear masses are taken from the mass evaluation [10] if available, otherwise predictions of RMF mass model [38] are employed. Panels (a)–(d) correspond to the neutron irradiation times $\tau_r = 1.5, 2.0, 2.5$, and 3.0 s, respectively.

It has been pointed out that the overestimation of half-lives in the FRDM + QRPA approach can at least partially be attributed to the omission of the $T = 0$ pairing [20]. This seems to be further confirmed in this work as the half-lives are systematically reduced with the inclusion of $T = 0$ pairing. For Cd isotopes with $N \geqslant 90$, however, the FRDM + QRPA calculation yields shorter half-lives than the RHFB + QRPA. The FRDM predicts a shape transition from the spherical ^{136}Cd to the deformed ^{138}Cd with quadrupole deformation $\beta_2 = 0.125$. This may indicate the shorter half-lives for Cd isotopes with $N \geqslant 90$ obtained in the FRDM + QRPA are due to the effect of nuclear deformation, which is not included in the present calculation. Similar systematics are also found for the Zr, Mo, Ru, Pd isotopes where shape transitions occur. However, it should be noted that a recent QRPA calculation that used a Skyrme interaction has shown the opposite trend [37]. Therefore, it will be interesting to include deformation degrees of freedom into the self-consistent QRPA calculations and study their effects on β-decay half-lives in the future.

To analyze the impact of the predicted β-decay half-lives on r-process abundances, we have also performed a classical r-process calculation similar to those of Refs. [39,40]. In this model, seed-nuclei (Fe) are irradiated by neutron sources of high and continuous neutron densities n_n over a timescale τ_r in a high temperature environment ($T \sim 1$ GK). As in Ref. [41], the components with neutron density $n_n = 10^{22}$–10^{24} cm^{-3} are used to investigate the impact of β-decay half-lives on the r-matter flow. The weight ω of each r-process component follows exponential relation on neutron density n_n:

$$\omega(n_n) = a \times n_n^b. \tag{9}$$

The parameters $a = 0.6435$ and $b = 0.0411$ are taken from the calculations in Ref. [40]. The abundances for each r-process component are calculated within the waiting-point approximation. In this model, the abundance distribution in an isotopic chain is given by the Saha equation and is entirely determined by neutron separation energies for a given temperature T (in this work, $T = 1.5$ GK) and a neutron density n_n. The nuclear β-decay rates control matter flow between neighboring isotopic chains. Therefore, in this model, the r-process path is only dependent on nuclear masses, from which neutron separation energies are determined. In this work, nuclear masses are taken from the mass evaluation [10] if available, otherwise predictions of RMF mass model [38] are employed. The corresponding r-process path is shown in Fig. 2.

Table 1
The half-lives of r-process bottleneck nuclei near $N = 82$ predicted by RHFB + QRPA and FRDM + QRPA approaches. For comparison, the experimental values [10] are also shown if available.

Nucleus	Half-life (s)		
	RHFB + QRPA	FRDM + QRPA	Exp.
^{124}Mo	0.0108	0.0106	–
^{126}Ru	0.0205	0.0342	–
^{128}Pd	0.0486	0.1251	–
^{130}Cd	0.1685	1.1232	0.162 ± 0.007
^{134}Sn	0.7530	3.5410	1.050 ± 0.011

In Fig. 4, we display four snapshots of r-process abundances at different neutron irradiation times τ_r. One notices that the half-lives calculated with RHFB + QRPA model (solid curves) produce a faster r-matter flow in the $N = 82$ region, and thus yield higher r-process abundances of nuclei with $A \gtrsim 140$. To understand this difference, the half-lives of nuclei forming the major bottlenecks of the r-matter flow (r-process bottleneck nuclei) near $N = 82$ are given in Table 1. Clearly, the experimental half-lives of ^{130}Cd and ^{134}Sn are better reproduced by RHFB + QRPA approach, while the FRDM + QRPA approach remarkably overestimates these half-lives. By merely replacing half-lives of ^{130}Cd and ^{134}Sn in the FRDM + QRPA approach by the corresponding RHFB + QRPA results, the calculated r-process abundances are shown by the dotted curves in Fig. 4. It is clear that the differences of the calculated abundances are mainly due to the differences of predicted half-lives of ^{130}Cd and ^{134}Sn between RHFB + QRPA and FRDM + QRPA approach. Furthermore, if we replace the FRDM + QRPA half-lives of all nuclei in Table 1 by the corresponding RHFB + QRPA results, almost the same abundances are obtained for nuclei around and beyond the second abundance peak. Moreover, by summing up the half-lives of r-process bottleneck nuclei near $N = 82$, one can roughly estimate the time when the r-process passes the second abundance peak. Based on the RHFB + QRPA results this

time is speeded up to 1.00 s, from the 4.83 s predicted by the FRDM + QRPA calculation. This is an important result for the estimate of the duration of the r-process, and hence the origin of heavy elements in the universe. In addition, using the RHFB + QRPA results, higher abundances are found at $A \sim 80$. This can easily be understood because it takes more time to pass the r-path nuclei ^{78}Ni and ^{80}Zn and, as a result, higher abundances are accumulated.

In summary, we have introduced a fully self-consistent proton–neutron quasiparticle random phase approximation (QRPA) for spherical nuclei, based on the relativistic Hartree–Fock–Bogoliubov (RHFB) framework. By employing an isospin-dependent proton–neutron $T = 0$ pairing interaction, the RHFB + QRPA model has been applied to a study of β-decay half-lives of neutron-rich nuclei with $20 \leqslant Z \leqslant 50$, extending over the entire r-process path from $N = 50$ to $N = 82$. It has been found that the RHFB + QRPA calculations reproduce the experimental β-decay half-lives for neutron-rich nuclei, especially for nuclei with half-lives less than one second. Using the calculated β-decay half-lives of neutron-rich nuclei a remarkable speeding up of r-matter flow has been predicted. This leads to an enhancement of r-process abundances of elements with $A \gtrsim 140$. It should be pointed out that the speeding up of r-matter flow mainly results from shorter half-lives of r-path nuclei close to $N = 82$, which are spherical or nearly spherical. Therefore, the spherical approximation in this work does not influence our key conclusions. Of course, to quantitatively reproduce the r-process abundances in the whole region the deformed QRPA approach should be employed, and we leave this further refinement for future consideration.

Acknowledgements

This work was partly supported by the Major State 973 Program 2013CB834400, the National Natural Science Foundation of China under Grant Nos. 10975008, 11105006, 11175001, 11175002, 11075066, and 11205004, the 211 Project of Anhui University under Grant No. 02303319-33190135, the Fundamental Research Funds for Central Universities under Contract No. lzujbky-2012-k07, the Program for New Century Excellent Talents in University of China under Grant No. NCET-10-0466, the Grant-in-Aid for JSPS Fellows under Grant No. 24-02201, and the MZOS-project No. 1191005-1010.

References

[1] D. Lunney, J.M. Pearson, C. Thibault, Rev. Mod. Phys. 75 (2003) 1021.
[2] E. Nácher, et al., Phys. Rev. Lett. 92 (2004) 232501.
[3] V. Tripathi, et al., Phys. Rev. Lett. 101 (2008) 142504.
[4] E.M. Burbidge, G.R. Burbidge, W.A. Fowler, F. Hoyle, Rev. Mod. Phys. 29 (1957) 547.
[5] Y.-Z. Qian, G.J. Wasserburg, Phys. Rep. 442 (2007) 237.
[6] K. Langanke, G. Martínez-Pinedo, Rev. Mod. Phys. 75 (2003) 819.
[7] C.S. Wu, E. Ambler, R.W. Hayward, D.D. Hoppes, R.P. Hudson, Phys. Rev. 105 (1957) 1413.
[8] I.S. Towner, J.C. Hardy, Rep. Prog. Phys. 73 (2010) 046301.
[9] H.Z. Liang, N. Van Giai, J. Meng, Phys. Rev. C 79 (2009) 064316.
[10] G. Audi, A.H. Wapstra, C. Thibault, Nucl. Phys. A 729 (2003) 337, updataed with data from National Nuclear Data Center, http://www.nndc.bnl.gov.
[11] P.T. Hosmer, et al., Phys. Rev. Lett. 94 (2005) 112501.
[12] J. Pereira, et al., Phys. Rev. C 79 (2009) 035806.
[13] S. Nishimura, et al., Phys. Rev. Lett. 106 (2011) 052502.
[14] P. Möller, J.R. Nix, K.-L. Kratz, At. Data Nucl. Data Tables 66 (1997) 131.
[15] N. Nishimura, T. Kajino, G.J. Mathews, S. Nishimura, T. Suzuki, Phys. Rev. C 85 (2012) 048801.
[16] E. Fermi, Z. Phys. 88 (1934) 161.
[17] G. Martínez-Pinedo, K. Langanke, Phys. Rev. Lett. 83 (1999) 4502.
[18] T. Suzuki, T. Yoshida, T. Kajino, T. Otsuka, Phys. Rev. C 85 (2012) 015802.
[19] I.N. Borzov, S. Goriely, Phys. Rev. C 62 (2000) 035501.
[20] J. Engel, M. Bender, J. Dobaczewski, W. Nazarewicz, R. Surman, Phys. Rev. C 60 (1999) 014302.
[21] I.N. Borzov, et al., Z. Phys. A 355 (1996) 117.
[22] J. Meng, H. Toki, S.G. Zhou, S.Q. Zhang, W.H. Longa, L.S. Geng, Prog. Part. Nucl. Phys. 57 (2006) 470.
[23] D. Vretenar, A.V. Afanasjev, G.A. Lalazissis, P. Ring, Phys. Rep. 409 (2005) 101.
[24] T. Nikšić, D. Vretenar, P. Ring, Prog. Part. Nucl. Phys. 66 (2011) 519.
[25] H.Z. Liang, P.W. Zhao, L.L. Li, J. Meng, Phys. Rev. C 83 (2011) 011302(R).
[26] N. Paar, T. Nikšić, D. Vretenar, P. Ring, Phys. Rev. C 69 (2004) 054303.
[27] T. Nikšić, T. Marketin, D. Vretenar, N. Paar, P. Ring, Phys. Rev. C 71 (2005) 014308.
[28] T. Marketin, D. Vretenar, P. Ring, Phys. Rev. C 75 (2007) 024304.
[29] H.Z. Liang, N. Van Giai, J. Meng, Phys. Rev. Lett. 101 (2008) 122502.
[30] H.Z. Liang, P.W. Zhao, J. Meng, Phys. Rev. C 85 (2012) 064302.
[31] W.H. Long, P. Ring, N. Van Giai, J. Meng, Phys. Rev. C 81 (2010) 024308.
[32] J.-P. Ebran, E. Khan, D. Peña Arteaga, D. Vretenar, Phys. Rev. C 83 (2011) 064323.
[33] J.F. Berger, M. Girod, D. Gogny, Nucl. Phys. A 428 (1984) 23.
[34] B. Cederwall, et al., Nature (London) 469 (2011) 68.
[35] B.S. Nara Singh, et al., Phys. Rev. Lett. 107 (2011) 172502.
[36] W.H. Long, N. Van Giai, J. Meng, Phys. Lett. B 640 (2006) 150.
[37] P. Sarriguren, J. Pereira, Phys. Rev. C 81 (2010) 064314.
[38] L.S. Geng, H. Toki, J. Meng, Prog. Theor. Phys. 113 (2005) 785.
[39] B. Sun, F. Montes, L.S. Geng, H. Geissel, Yu.A. Litvinov, J. Meng, Phys. Rev. C 78 (2008) 025806.
[40] Z.M. Niu, B. Sun, J. Meng, Phys. Rev. C 80 (2009) 065806.
[41] P. Möller, B. Pfeiffer, K.-L. Kratz, Phys. Rev. C 67 (2003) 055802.